

Electron-impact excitation of the $^3S^0$ and $^5S^0$ states of atomic oxygen

E. J. Stone and E. C. Zipf

Department of Physics, University of Pittsburgh, Pittsburgh, Pennsylvania 15260

(Received 10 May 1973)

Absolute cross sections for the excitation of the OI $3s(^3S^0)$ and $3s(^5S^0)$ states by electron impact on atomic oxygen have been measured for electron energies from threshold to 300 eV. The magnitude of the $^3S^0$ cross section is $5.3 \times 10^{-17} \text{ cm}^2 \pm 40\%$ at its peak at 20 eV. This cross section differs in magnitude and shape from the result reported earlier. The $^5S^0$ cross section has a maximum value of $2.5 \times 10^{-17} \text{ cm}^2 \pm 50\%$ at 15 eV. Both cross sections are larger than the values predicted by recent theoretical calculations. The experimental techniques used in the production of atomic oxygen and in the measurement of the OI density have been improved and are described in detail. Critical experimental problems concerning the loss of atoms at the system walls and the role of excited states of O_2 in the discharged gas are also discussed.

INTRODUCTION

The 1304 Å ($^3P - ^3S^0$) and 1356 Å ($^3P - ^5S^0$) emissions of atomic oxygen are prominent features in the spectra of the day airglow, the polar aurora, the tropical ultraviolet airglow of the Earth, and the sunlit atmosphere of Venus and Mars. The relative intensities of these two features vary considerably among these phenomena, indicating that the mechanisms or circumstances of excitation are probably different. Electron-impact excitation is one of the chief mechanisms proposed to explain this emission, but until recently little reliable information has been available on the pertinent cross sections.

The cross section for excitation of the OI($\lambda 1304$ Å) resonance triplet in electron impact on atomic oxygen has been reported in an experimental measurement by the authors¹ and in several theoretical calculations.²⁻⁵ These results have differed substantially on both the magnitude and shape of the cross section. Because of the importance of this cross section to the study of planetary atmospheres, we have continued our work on this measurement in an attempt to reduce various uncertainties which were present in our preliminary study. We report here a revised total cross section for the excitation of $\lambda 1304$ Å radiation which is lower in magnitude and less sharply peaked than that reported earlier. We have also measured the cross section for excitation of the $\lambda 1356$ Å emission, assigning it an absolute magnitude based on optical data and a calculation of the signal loss due to the thermal motion of the excited atoms.

EXPERIMENTAL

The basic apparatus was the same as that described in detail previously,¹ with a few modifications. Gas flowed along a delivery tube and into a small collision chamber located in a large, rapidly pumped vacuum chamber (see Fig. 1). An electron beam from an electrostatically focused electron gun passed through the chamber and was collected on the opposite side. The electron energy could be varied from 8 to 340 eV; the energy spread of the beam was less than 2 eV. Current to the electron collector and stray currents to the walls of the collision chamber were monitored with electrom-

eters. Radiation emitted within the chamber was observed at right angles to the electron beam through an aperture in the collision chamber with a 1-m normal-incidence vacuum monochromator and solar-blind photomultiplier tube operated in a pulse-counting mode. Pressures in the collision chamber and large vacuum chamber were measured with an ionization gauge that was calibrated against a McLeod gauge. Oxygen atoms were produced in the flowing gas by means of a microwave discharge in the gas delivery tube. The density of oxygen atoms in the collision chamber was determined by observing the absorption of OI($\lambda 1302.2$ Å) resonance radiation within the chamber. This resonance radiation was produced as an impurity emission line in an rf discharge in helium placed on the opposite side of the collision chamber from the monochromator.

The experiment was conducted by counting photons with the discharge off and on, alternately. The counting period was 30 sec in each mode, which was short enough to hold drifts in the gas pressure and electron beam current to 1% or 2% at most. The difference in photon count rate per unit of electron beam current per unit of pressure, with corrections for O_2 loss and O_2 excitation (see the following discussion), was taken to be the contribution from direct electron-impact excitation of atomic oxygen.

The following modifications were incorporated in our original apparatus to improve the basic experiment. The first change was the introduction of a constriction in the gas flow tube just downstream from the microwave discharge (see Fig. 1). This permitted the discharge to run at higher pressures than before and increased the percentage of dissociated oxygen. The electron impact experiment thus could be run at lower total pressures than was formerly possible in order to reduce the interaction of the electron beam with the oxygen gas. At electron energies of 100 eV, the difference between the discharge-on and discharge-off signals was about 15%, compared with 3%–5% previously.

A new photomultiplier tube (EMR 541GX) with a quantum efficiency about 3 times that of the old one was installed, thus significantly improving the counting statistics.

The light source used for the atomic density measurements was redesigned to ensure optical thinness.⁶

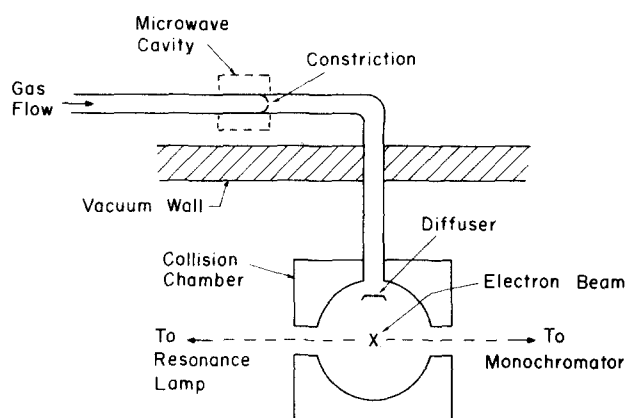


FIG. 1. Diagram of the experimental apparatus.

The thinness of the atomic oxygen resonance lines in the source was verified by observing the relative intensities of the three lines of the triplet, which should appear in the ratios 5:3:1 in the absence of self-reversal. A sample scan of the resonance triplet is shown in Fig. 2. Summing the areas under the three peaks in this scan and several other scans taken periodically during the absolute cross section determination gave an average of 4.7:2.9:1.0 for the relative intensities. This deviation from the ideal ratios causes an (upward) error in the determined absolute value of the cross section. From the discussion of such errors by Kaufman and Parkes⁷ we conclude that this error is about 2%. The reported result is corrected accordingly.

The resonance absorption measurement of atomic density is based on knowledge of the oscillator strength of the $Or(^3P - ^3S^0)$ transition. The most recent measurements of this oscillator strength are those of Lin, Parkes, and Kaufman⁸ ($f=0.046$), Lawrence⁹ ($f=0.046$), and Ott¹⁰ ($f=0.049$). Theoretical values for this oscillator strength, such as that calculated by Kazaks, Ganas, and Green³ and others cited in their paper, considerably exceed the experimental results. We have adopted the experimental result ($f=0.047$), noting that our atom density measurement procedure is just the inverse of that used in one of the oscillator strength measurements.⁸ (Ironically, choosing an oscillator strength more in agreement with Kazaks *et al.* would worsen the agreement between our measured and their calculated cross sections).

The emission and absorption line shapes were assumed to have thermal Doppler profiles for temperatures of 400 and 320 °K, respectively (see Ref. 6). The relation between absorption and atom density was computed from the formulas of Mitchell and Zemansky.¹¹ The observed absorption varied from 2% to 15%, depending on gas pressure.

The optical signal due to direct excitation of atoms was corrected for absorption by ambient atoms within the collision chamber. The signal from dissociative excitation of O_2 was not corrected for this effect, since the high velocities of excited atoms produced in dissociation cause an emission line shape which is very broad compared to the absorption line shape. Poland and

Lawrence¹² report that this width is 35–70 times the thermal Doppler width.

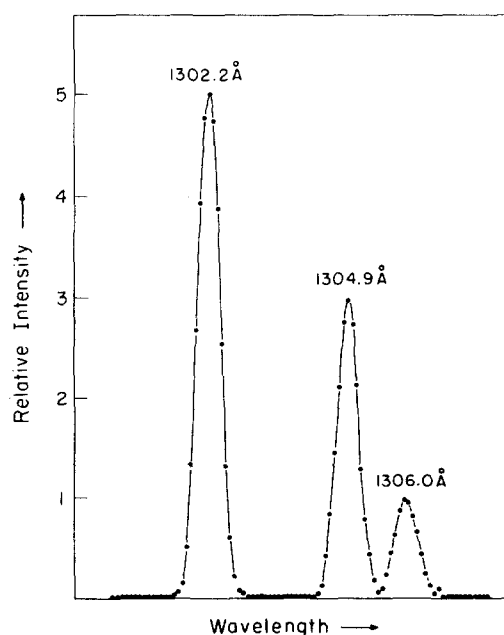
In order to produce a substantial atomic signal, a small fraction (~2%) of H_2 was introduced into the flowing O_2 before it passed through the discharge. The H_2 greatly increased the dissociation fraction in the oxygen (about an order of magnitude in our case), and is believed to act as a catalyst¹³ or to provide a coating on the walls of the flow tube which inhibits atom loss.¹⁴ Helium and argon were also mixed with the oxygen in varying concentrations in an attempt to provide a high dissociation fraction in the experimental region, but without success. N_2 was also rejected as a carrier gas because of problems arising from formation of nitrogen oxides and from contamination of the optical signals by the LBH band system of N_2 .

The cross section for the $Or(^3S^0)$ excitation reported here is approximately a factor of 2 below the result reported previously.¹ The difference is believed to be due to a fault in a now discarded electronic counter. The fault caused an underestimate of the atom density in the collision chamber and thus an erroneously large cross section.

THE DISCHARGED GAS

Unwanted molecules

With the microwave discharge turned off, the gas flowing through the collision chamber consists of ground state $O_2(^3\Sigma_g^-)$ molecules and a small fraction (about 2%) of H_2 molecules. With the discharge turned on, the gas may contain atomic oxygen and hydrogen, excited states of molecular oxygen, and a variety of hydrogen oxides, along with ground state O_2 and H_2 . The only added species desired, of course, is atomic oxygen. It is therefore important to assess the affect on the optical signal of other species which may be present.

FIG. 2. Scan of the $Or(\lambda\lambda\ 1302.2, 1304.9, 1306.0\ \text{\AA})$ resonance multiplet produced in the optically thin light source.

The most likely contaminant is $O_2(^1\Delta_g)$, which has been observed in the afterglow of oxygen discharges in concentrations as high as 10%,^{15,16} and which is long lived with respect to wall de-excitation. Another metastable molecule, $O_2(^1\Sigma_g^+)$, may appear in concentrations at least an order of magnitude smaller.¹⁷ Other discharge-produced species which can result in OI radiation by dissociative excitation include water, ozone, and vibrationally excited ground state O_2 . Thus it is important to assess the effect which these unwanted species have on the optical signal produced from the discharged gas.

One obvious test of the effect of unwanted molecular species is to examine the difference between the discharge-on and discharge-off signals when oxygen atoms are deliberately eliminated from the discharged gas. To produce this situation a tube of aluminum foil was placed in the flow tube downstream from the discharge. The metal surface causes rapid recombination of the oxygen atoms, but has relatively little effect on metastable molecules.¹⁶ The removal of atoms appeared in the experiment as complete loss of the discharge-on 1304 Å signal at energies below the threshold for dissociative excitation of O_2 . At higher electron energies there was no distinguishable difference between the discharge-on and discharge-off optical signals, indicating that molecular species not removed by the foil had negligible effect on the 1304 Å signal.

Another method for the elimination of atoms was discovered accidentally. When an electrodeless rf discharge was formed just downstream from the microwave discharge, the low-energy atomic signal was reduced by a factor of about 20. One explanation for this observation is that the relatively high-energy electrons produced by the rf discharge succeeded in ionizing most of the atoms, which were then quickly removed by wall collisions. Another possibility is that the rf discharge simply cleaned the Pyrex wall efficiently, allowing a greatly increased wall loss rate for neutral atoms. In this test also, the difference between the discharge-on and discharge-off signals at higher electron energies was just that which would be expected due to surviving atoms, within the limits of statistical error.

We conclude from these tests of the effect of atom removal that although molecular contaminants [especially $O_2(^1\Delta_g)$] were probably present in the discharge gas, their contribution to the 1304 Å signal is approximately equivalent to the contribution from the ground state O_2 from which they were formed.

Cook *et al.*¹⁸ have recently investigated the degree of vibrational excitation in the afterflow of a microwave discharge in O_2 and found vibrational temperatures of 600° K and lower. This result indicates that only a small fraction (<0.023) of the $O_2(^3\Sigma_g^-)$ molecules are in vibrational states above $v=0$. Thus it is unlikely that vibrational excitation of O_2 contributes significantly to the difference between the discharge-on and discharge-off optical signals.

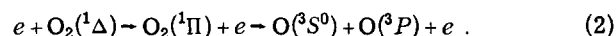
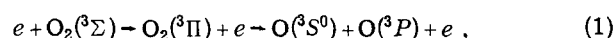
Further evidence that the difference between the discharge-off and discharge-on optical signals is due to atomic oxygen is the experimental fact that the difference

signal rises rapidly and smoothly from the expected threshold (9.5 eV) to its peak at 20 eV. Differences in optical signal due to dissociative excitation of new molecular species would be characterized by a later, gentler onset and a peak magnitude in the region 50–100 eV.

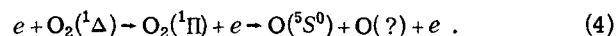
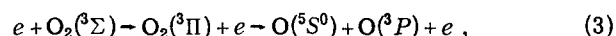
We have therefore interpreted the data from the $^3S^0$ ($\lambda 1304$ Å) excitation as though the presence of any molecules other than $O_2(^3\Sigma_g^-)(v=0)$ had no effect on the optical signal. However, we were not able to make the same assumption in analyzing the $^5S^0(\lambda 1356$ Å) data.

A very interesting phenomenon was observed in the course of measuring the excitation function for the 1356 Å emission. Above electron energies of about 35 eV, the discharge-on signal was *less* than the discharge-off signal, even after accounting for the O_2 pressure difference. This result implies that the probability for dissociatively exciting the $^5S^0$ state is lower in discharged O_2 than in the undisturbed gas. The analysis of the data was carried out by assuming that at high electron energies, the cross section should approach zero rapidly, since the transition is spin forbidden. The discharge-off signal was multiplied by a fixed ad hoc factor (usually about 0.90) to achieve this result before the discharge-on and discharge-off signals were subtracted.

We interpret this phenomenon as due to the presence of $O_2(^1\Delta_g)$ in the discharge gas. Although none of the cross sections for dissociative excitation of $O_2(^1\Delta_g)$ is known, it is possible to make a qualitative explanation of the phenomenon using selected rules for dipole-allowed transitions. The excited OI($^3S^0$) atom can be produced from both the $^3\Sigma$ and $^1\Delta$ states of the O_2 molecule, leaving the second fragment in the ground OI(3P) state,



On the other hand, production of OI($^5S^0$) is distinctly easier from the ground state,



Reaction (4) can only proceed by the production of an excited quintet state as the second fragment and thus requires almost twice as much energy as Reaction (3). [Of course, Reaction (3) can proceed in an equivalent manner, producing two excited triplet states.] Thus, while Reactions (1) and (2) seem to have approximately equal likelihood, it is plausible that the cross section for Reaction (4) is considerably less than that for Reaction (3).

Atom loss at walls

Another critical consideration is the probability that an oxygen atom formed in the discharge will be lost at the walls of the flow system, as well as the nature of this loss process. Experiments designed to determine the probability of atom loss per atom-wall collision have produced widely divergent results. Experiments

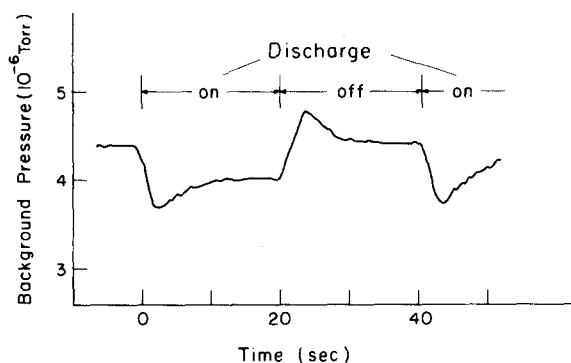


FIG. 3. Variation of background pressure in large vacuum chamber as the discharge was turned on and off.

conducted at low pressure in an ac mode find this probability to be on the order of 0.5 for common laboratory surfaces.^{19,20} Experiments at higher pressures in a dc mode find this probability to be two to four orders of magnitude smaller.^{21,22}

In the present experiment, oxygen atoms encounter unbaked surfaces of glass (Pyrex) and graphite (the interior of the collision chamber is painted with a Dag dispersion). Since oxygen atoms survived to be observed in the collision chamber, it is clear that the probability for loss on Pyrex was low. In earlier work, it was calculated that the loss probability on graphite was sufficiently low (< 0.2) to provide an essentially isotropic distribution of atoms in the collision chamber. We have confirmed this conclusion experimentally by inserting a Teflon diffuser in the path of the gas entering the collision chamber (see Fig. 1). Data taken with and without the diffuser indicate that its use was unnecessary, since the relation between resonance absorption and the electron impact atomic excitation signal remained the same.

In their pulsed-beam experiment, which found high atom loss probabilities, Riley and Giese²⁰ reported that atom loss at the test surfaces did not appear to be recombination to O_2 , but simple collection of the atoms by the wall. We find confirmation of this result in the fact that a drop in background pressure occurred in the system when the dissociating discharge was turned on. The observed drop was too great to be due to formation of hydrogen oxides from H_2 and O_2 and seemed to imply that atoms lost at the system walls were not returned to the gas phase in a time which was much less than a few minutes. That is, we could not assume that the total amount of oxygen, in atomic and molecular forms, flowing through the collision region was constant.

The pressure drop had two components, short term and steady state. The variation in system background pressure as the discharge was turned on and off is illustrated in Fig. 3. The short-term drop lasted about 10 sec and was avoided simply by waiting between counting periods. The steady state background pressure drop occurred only in O_2 in the presence of H_2 . It did not occur when nitrogen or argon was substituted for the oxygen, and was greatly diminished if the H_2 supply was shut off. The short-term drop occurred in all three gases, although it was greatest in oxygen. We interpret

the long-term pressure drop as being due to real and permanent loss of oxygen from the discharged gas. We suspect that the short-term variation was due to varying charge formations on the walls of the delivery tube affecting the flow of ions.

In reaching the results previously reported,¹ it was assumed that the total rate of oxygen mass flow through the collision chamber was not altered by the discharge, since no mechanism seemed available to change the flow rate through the inlet leak valves or the efflux from the collision chamber. Also in the earlier measurements, the fractional change in the background pressure was much smaller and was concealed in the random pressure variations of the diffusion-pumped system. This was because the constriction in the delivery tube was not used, and thus the total oxygen flow rate was much higher, and the degree of dissociation lower, than in the later measurements. We thus assumed that molecular oxygen was lost from the discharge afterflow only to the extent that atomic oxygen was present.

However, a study of the relation between the optical signal from electron impact and the background pressure as a function of time after the discharge was turned on or off left no doubt that the loss of oxygen in the discharge-on mode was real. The present results are based on the assumption that the fractional loss of molecular oxygen is directly proportional to the fractional change in the background pressure in the large vacuum chamber, after subtracting that portion of the background pressure not due to flow of the experimental gas. The difference in the shape of the cross section between our present and previous results is chiefly due to this difference in the interpretation of the data and to the increased dissociation fraction in the discharged gas.

RESULTS

$O(^3S^0)$

The result of the absolute cross section determination is that the cross section for excitation of the $^3S^0$ state in electron impact on atomic oxygen at 14 eV is 11.4 times the cross section for dissociative excitation of the same state in electron impact on molecular oxygen at 100 eV.

The latter cross section has been measured by Mumma and Zipf²³ as $3.8 \times 10^{-18} \text{ cm}^2 \pm 17\%$, by Ajello²⁴ as $3.0 \times 10^{-18} \text{ cm}^2 \pm 10\%$, and by Lawrence⁹ as $3.05 \times 10^{-18} \text{ cm}^2 \pm 15\%$. We have repeated the measurement of Mumma and Zipf in the course of this work, using a spectral sensitivity determination based on the LBH bands of N_2 ²⁵ and Lyman band fluorescence in HD,²⁶ and found a value of $4.2 \times 10^{-18} \text{ cm}^2 \pm 15\%$. Using the mean value of $3.5 \times 10^{-18} \text{ cm}^2$ for the dissociative cross section, we have a value of $5.3 \times 10^{-17} \text{ cm}^2 \pm 40\%$ for the direct excitation cross section at its peak at 20 eV. The 40% error estimate is considered to be total probable error, including both statistical and systematic sources.

The cross section for excitation of the $^3S^0$ state as a function of electron energy is shown as the data points in Fig. 4. The error bars represent ± 1 standard deviation in the statistical error. Numerical values for

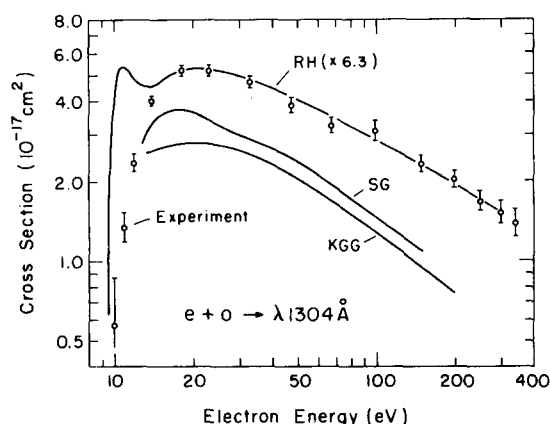


FIG. 4. Cross section for electron-impact excitation of the $^3S^0$ state in atomic oxygen. Circles with error bars: this work; RH, Rountree and Henry (Ref. 5) multiplied by 6.3; KGG, Ganas and Green (Ref. 3); SG, Sawada and Ganas (Ref. 4).

these points are given in Table I.

The cross sections reported here are total cross sections for electron-impact excitation, including all fast cascade transitions, calculated on the assumption that the resulting radiation is distributed isotropically in space. This assumption is justified, since the upper states involved are spherically symmetric S states.

Recent theoretical results are also shown in Fig. 4 for comparison. The curve KGG is the sum of the excitation cross sections for the $3s(^3S^0)$ and $3p(^3P^0)$ levels obtained by Kazaks *et al.*³ The curve SG is the higher of two slightly different cross sections reached by Sawada and Ganas,⁴ and includes cascade contributions from the $3p(^3P^0)$ and $4p(^3P^0)$ levels. The curve RH is the result of Rountree and Henry,⁵ multiplied by a factor of 6.3. The first two theoretical results mentioned lie near the lower limits of the stated probable error for the experimental result reported here. We note that the $3s(^3S^0)$ state is in fact populated by weak cascade transitions from a large number of high-lying triplet states. Inclusion of these contributions to the total cross section would raise the theoretical results somewhat and thus would improve the agreement with the experimental result.

We do not observe the low-energy resonancelike peak in the cross section of Rountree and Henry, although at higher energies the agreement in shape is good. Aside from the fact that they make no attempt to include cascade contributions to the cross section, we have no explanation of the large difference in magnitude between our cross section and theirs.

It should be noted that all these theoretical results are based on a frozen-core approximation in which it is assumed that the configuration underlying the active electron is always $^4S^0$. In work presently underway, we have observed substantial emission from the 989 Å transition in electron-impact excitation of atomic oxygen. The upper state of this transition has a $^2D^0$ core. Presumably, taking account of coupling to underlying configurations other than $^4S^0$ will also raise the values of the theoretical cross sections somewhat.

O($^5S^0$)

The ratio of the peak cross sections for excitation of the $^5S^0$ and $^3S^0$ states was determined from the ratio of the observed optical signals in the following way. For a number density of atomic oxygen in the collision chamber n , electron beam current I , and excitation cross section σ , the number of excited states produced per unit length of the beam per unit time is $nI\sigma$. If the radiative lifetime of these states is short (less than 10^{-7} sec) as for the $^3S^0$ state, the atoms will radiate before they have moved out of the field of view of the monochromator. If the lifetime is relatively long, as for the $^5S^0$ state, some of the excited states will move out of the field of view before radiating. For a lifetime τ the density ρ of excited states as a function of distance x from the electron beam is given by

$$\rho(x) = nI\sigma J, \quad (5)$$

where

$$J = \int_{-l}^l \int_0^\infty \frac{P(v)e^{-D/v\tau}}{4\pi D^2 v} dv dz, \quad (6)$$

where v is the atom's speed, D is the distance between the point of excitation and the point of observation, $2l$ is the length of the electron beam within the collision chamber, and z indicates position along the electron beam, as illustrated in Fig. 5. $P(v)$ is the Maxwell-Boltzmann scalar velocity distribution

$$P(v) = 4\pi \left(\frac{m}{2\pi kT} \right)^{1.5} v^2 \exp \left(-\frac{mv^2}{2kT} \right), \quad (7)$$

where m is the mass of the oxygen atom, T is the Kelvin temperature, and k is Boltzmann's constant.

The photon emission rate from the volume V of the collision chamber viewed by the monochromator is then

$$E = A \int_V \rho dV = nI\sigma A \int_V J dV, \quad (8)$$

where $A = 1/\tau$ is the Einstein radiative transition probability. The ratio of excitation cross sections is then given by

TABLE I. Measured cross section for excitation of O($^3S^0$).

Electron energy (eV)	Cross section (10^{-17} cm ²)	Statistical error
10	0.6	50%
11	1.4	20%
12	2.4	10%
14	4.0	2%
18	5.3	3%
23	5.2	4%
33	4.7	5%
48	3.9	6%
70	3.2	7%
100	3.1	8%
150	2.3	9%
200	2.0	10%
250	1.7	10%
300	1.5	12%
340	1.4	12%

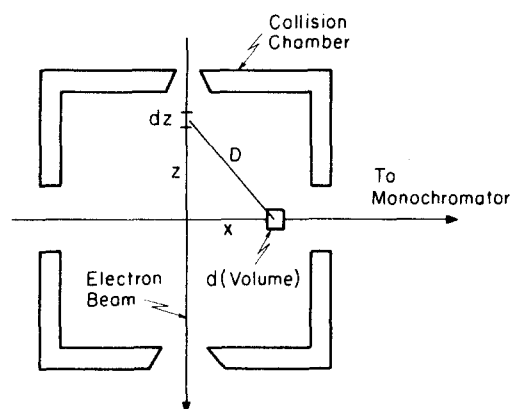


FIG. 5. Geometry of the collision chamber, showing parameters used in the calculation of the spatial distribution of $O(^5S^0)$.

$$R = \frac{\sigma(^5S^0)}{\sigma(^3S^0)} = \frac{s(^5S^0)}{s(^3S^0)} \left(A(^5S^0) \int J dV \right)^{-1}, \quad (9)$$

where s denotes optical signal (photon counting rate) for the two transitions under identical experimental conditions. Vignetted regions of the collision chamber were small and were included in the calculation in an approximate way. The sensitivity of the optical system was the same at the two wavelengths observed.

The lifetime of the $O(^5S^0)$ state has been calculated by Nicolaidis²⁷ as 192 μsec (with no estimate of error), measured in time-of-flight experiments by Johnson²⁸ as $185 \pm 10 \mu\text{sec}$ and by Wells and Zipf²⁹ as $189 \pm 50 \mu\text{sec}$, and measured by Ott³⁰ in an experiment observing line emission in a cascade arc as $146 \mu\text{sec} \pm 40\%$. We have

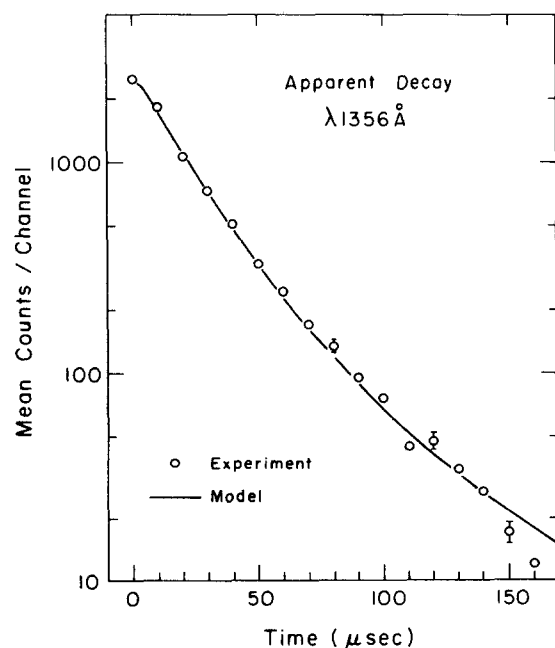


FIG. 6. Decay of $\lambda 1356 \text{ Å}$ radiation after electron beam shut-off as viewed through collision chamber aperture, compared with calculated decay based on assumption of complete de-excitation in wall collisions.

used the value of 180 μsec in our calculation.

The calculation is based on the assumption that no $O(^5S^0)$ atoms survive collision with the walls of the experimental chamber, and that gas collisions may be ignored. The O_2 pressure in the collision chamber during the measurement was about 2×10^{-4} torr, implying a mean free path, at least for ground state species, in excess of 20 cm. The distance from the electron beam to the cylindrical chamber wall was 2.5 cm. The assumption of complete $^5S^0$ de-excitation in wall collisions was tested by pulsing the electron beam on and off in a square-wave pattern and observing the decay of 1356 Å radiation after beam shutoff. This decay was compared with a computer model of the decay, a variation of the calculation described above. [In integral (6), for distance D and time t after shutoff, permit no velocities greater than D/t .] The experiment and the model are shown in Fig. 6, and the agreement is seen to be good.

The integrals in Eq. (5) and (8) were evaluated numerically. The ratio of optical signals from $\lambda 1304 \text{ Å}$ and $\lambda 1356 \text{ Å}$ was measured at an electron energy of 14 eV. The resulting value of R was 0.62. Thus the peak value for the $^5S^0$ cross section is $2.5 \times 10^{-17} \text{ cm}^2 \pm 30\%$ at an electron energy of 15 eV. The error estimate represents possible error in the measurement and the calculation, relative to the value of the peak $^3S^0$ cross section.

The measured cross section for direct excitation of $O(^5S^0)$ as a function of electron energy, determined as described above, is shown in Fig. 7. Error bars represent ± 1 standard deviation in the statistical error. The reproducibility of the data was poor at higher electron energies; the shaded area of the graph indicates the extent of variation in several data runs. Two points from the theoretical work of Sawada and Ganas⁴ are shown. Again, the experimental values exceed the theoretical ones.

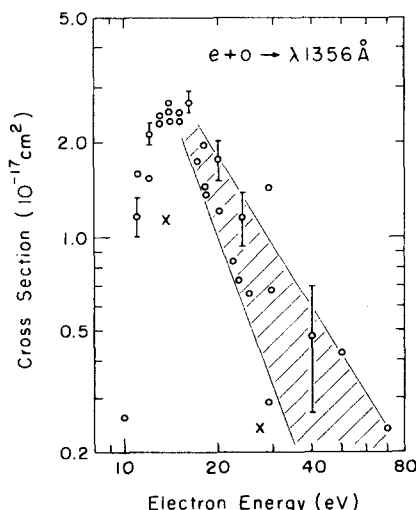


FIG. 7. Cross section for electron-impact excitation of the $^5S^0$ state in atomic oxygen. Circles, this work; crosses, Sawada and Ganas (Ref. 4).

SUMMARY

The conditions of electron-impact excitation in flowing oxygen downstream from a discharge have been reinterpreted. The data indicate that total oxygen mass flow is not conserved as the discharge is turned on and off, even though the inlet flow rate remains constant. The total amount of gas is diminished when the discharge is turned on, apparently due to collection of atomic oxygen by the system walls.

The revised cross section for excitation of $O(^3S)$ in electron impact on atomic oxygen is lower in magnitude and less sharply peaked than that reported previously.

A calculation of the spatial distribution of metastable $O(^5S^0)$ in the collision chamber, together with a comparison of the 1356 and 1304 Å optical signals, enabled the experiment to yield a cross section for excitation of this state also.

ACKNOWLEDGMENTS

This research was supported in part by the National Aeronautics and Space Administration (NGL 39-011-030) and by the Advanced Research Projects Agency, The Department of Defense, and was monitored by the U.S. Army Research Office, Durham, under Contract No. DA-31-124-ARO-D-440.

¹E. J. Stone and E. C. Zipf, Phys. Rev. A **4**, 610 (1971).

²A. D. Stauffer and M. R. C. McDowell, Proc. Phys. Soc. (Lond.) **89**, 289 (1966).

³P. A. Kazaks, P. S. Ganas, and A. E. S. Green, Phys. Rev. A **6**, 2169 (1972).

⁴T. Sawada and P. S. Ganas, Phys. Rev. A **7**, 617 (1973).

⁵S. P. Rountree and R. J. W. Henry, Phys. Rev. A **6**, 2106

(1972).

⁶E. J. Stone and E. C. Zipf, J. Chem. Phys. **58**, 4278 (1973).

⁷F. Kaufman and D. A. Parkes, Trans. Faraday Soc. **66**, 1579 (1970).

⁸C. L. Lin, D. A. Parkes, and F. Kaufman, J. Chem. Phys. **53**, 3896 (1970).

⁹G. M. Lawrence, Phys. Rev. A **2**, 397 (1970).

¹⁰W. R. Ott, Phys. Rev. A **4**, 245 (1971).

¹¹A. C. G. Mitchell and M. W. Zemansky, *Resonance Radiation and Excited Atoms* (Cambridge U. P. Cambridge, England, 1934), pp. 92–122 and 323.

¹²H. M. Poland and G. M. Lawrence, J. Chem. Phys. **58**, 1425 (1973).

¹³F. Kaufman and J. R. Kelso, J. Chem. Phys. **32**, 301 (1960).

¹⁴F. Kaufman, Advan. Chem. Ser. **80**, 29 (1969).

¹⁵S. N. Foner and R. L. Hudson, J. Chem. Phys. **25**, 601 (1956).

¹⁶L. Elias, E. A. Ogryzlo, and H. I. Schiff, Can. J. Chem. **37**, 1680 (1959).

¹⁷J. F. Noxon, Can. J. Phys. **39**, 1110 (1961).

¹⁸T. J. Cook, B. R. Zegarski, W. H. Breckenridge, and T. R. Miller, J. Chem. Phys. **58**, 1548 (1973).

¹⁹G. S. Hollister, R. T. Brackmann, and W. L. Fite, Planet. Space Sci. **3**, 162 (1961).

²⁰J. A. Riley and C. F. Giese, J. Chem. Phys. **53**, 146 (1970).

²¹J. W. Linnett and D. G. H. Marsden, Proc. R. Soc. A **234**, 489 (1956).

²²G. A. Melin and R. J. Madix, Trans. Faraday Soc. **67**, 198 (1971).

²³M. J. Mumma and E. C. Zipf, J. Chem. Phys. **55**, 1661 (1971).

²⁴J. M. Ajello, J. Chem. Phys. **55**, 3156 (1971).

²⁵M. J. Mumma and E. C. Zipf, J. Opt. Soc. Am. **61**, 83 (1971).

²⁶E. J. Stone and E. C. Zipf, J. Chem. Phys. **56**, 4646 (1972).

²⁷C. A. Nicolaides, Chem. Phys. Lett. **17**, 436 (1972).

²⁸C. E. Johnson, Phys. Rev. A **5**, 2688 (1972).

²⁹W. C. Wells and E. C. Zipf, Trans. Am. Geophys. Union **53**, 459 (1972).

³⁰W. R. Ott (private communication).